ARMA 21–2076

Evaluation of SLAM-Based Mobile LiDAR Workflows and Data Quality for Mine-Wide Underground Geotechnical Monitoring

Lukas Fahle[1], Pete Carney[2], Scott Schiele[2], Gabriel Walton, PhD[1], Elizabeth Holley, PhD[1]

[1]*Colorado School of Mines, Golden, CO, USA*

[2]*Mine Vision Systems, Pittsburgh, PA, USA*

ABSTRACT: Adverse ground behavior is a hazard to both personnel and non-human assets in any underground mine. Traditional visual inspections and embedded or static instruments are not well-suited for mine-wide digital data collection and geotechnical monitoring. This paper investigates emerging Simultaneous Localization and Mapping (SLAM)-based Light Detection and Ranging (LiDAR) scanning as a mobile remote sensing technology that can efficiently enable collection of mine-scale digital data. Based on experiments in two underground mines using two state-of-the-art mobile mapping systems (MMS), the authors describe collection and processing workflows. The authors then analyze the results on a target- and site-level to highlight the differences, limitations, and benefits of MMS data versus traditional static LiDAR scanning data. The investigated quality metrics include visual data quality, accuracy (trueness and precision), coverage, density, and SLAM-drift. The paper concludes with a discussion of workflows and data quality in the context of mine-wide geotechnical monitoring and gives recommendations for future research efforts.

1. INTRODUCTION

Adverse ground behavior events, such as convergence and fall of ground, represent hazards to both personnel and non-human assets in US and international underground coal, metal, and nonmetal mines (Kaiser and Cai, 2012; Mark and Molinda, 2004; Nordlund, 2013; Palei and Das, 2008; Sandbak and Rai, 2013). Monitoring of ground response to mining activities is crucial to ensure safety, operational reliability, and economic viability of underground mine sites – a fact which will only become more prominent with increasing depth of mines, more challenging ground conditions, and less personnel at the face (Fairhurst, 2017).

Traditional geotechnical monitoring relies heavily on in-person, visual inspections by specialists, resulting in analog and qualitative data of variable and low accuracy. Data accuracy is described by both trueness (i.e., "the closeness of agreement between the arithmetic mean of a large number of test results and the true or accepted reference value" and precision (i.e., "the closeness of agreement between test results") as defined by ISO (2021). Therefore, frequent and comprehensive mine-wide visual inspections are often neither economically feasible nor do they deliver technically robust data. To augment visual inspections, embedded and stationary geotechnical instruments, such as multi-point borehole extensometers and tripod-mounted instruments (e.g., total stations, LiDAR) can be deployed. While they can collect data with much higher trueness and precision at a higher cost, they are often not suitable for economic mine-wide monitoring as they lack the required spatial and temporal resolution.

Non-embedded, mobile mapping systems (MMS) using (among others) Light Detection and Ranging (LiDAR) sensors and Simultaneous Localization and Mapping (SLAM) algorithms can enable the frequent acquisition of rich, digital data sets on a mine-wide scale (Zlot and Bosse, 2014). While unmanned aerial vehicle (UAV)-based LiDAR scanning is now standard for volumetric surveys of mine areas with limited accessibility (e.g., stopes) (Jones et al., 2020), mine-wide applications for mapping, change detection, and monitoring are still in their early stages.

The following sections illustrate the data collection and processing workflows for this novel technology. The authors evaluate local and global data quality characteristics such as trueness, precision, density, and coverage based on two different data sets collected with two SLAM-based MMSs in two underground mines.

2. SLAM-LIDAR INSTRUMENTATION, DATA COLLECTION, AND PROCESSING WORKFLOWS

The high-level workflows for static and MMS LiDAR geotechnical monitoring are very similar to each other. The following sections describe some unique aspects of work scope, instrumentation, data collection, and processing to highlight the importance of understanding this novel technology's applicability.

2.1. Work Scope

Before any MMS (or geotechnical instrument) is deployed, a scope of work including a risk assessment for the monitored area, its size, expected types and magnitudes of changes, required frequency of monitoring, and operational constraints should be clearly defined. With this knowledge, the minimum achievable data quality that an MMS must deliver and the need for other relevant product features such as versatility of deployment, robustness, and software capabilities can be identified. Based on a work scope and minimum instrument requirement, MMS can be vetted and selected for further testing and regular operational deployment.

2.2. Mobile Mapping Systems

Mobile mapping systems (MMSs) have been implemented on various platforms such as airplanes, helicopters, UAVs, automotive vehicles, boats, and backpacks (Williams et al. 2013). Most MMSs are made up of five components: mobile platform, positioning hardware, laser scanner(s), photographic/video recording, and computer and data storage (Puente et al. 2013). The newest generation of commercial SLAM-based compact mapping systems (e.g., Kaarta Stencil 2 and Emesent Hovermap) utilizes automotive-grade LiDAR sensors in conjunction with an Inertial Measurement Unit (IMU) to generate 3D-point cloud maps in real-time while estimating the system's position within this map. Such units can be mounted to various mobile platforms or used handheld. (Emesent, 2021; Kaarta, 2021)

2.3. Data Collection

For frequent deployment over multi-kilometer long mapping trajectories, a ground-based mobile platform such as a light mine utility vehicle is the preferred mobile platform. The MMS should be mounted so that obstructions of the line-of-sight of the sensor are minimized, and the sensor faces in the direction of travel.

During data collection, speed should be kept constant and in the range of 5 to 8 km/h to ensure uniform and dense sampling of the mine drift wall. Higher driving speeds are possible but will reduce the point cloud density. To improve the repeatability of scans, the environment should also be traversed, following the same trajectory for each scan epoch.

2.4. Data Processing

Like static LiDAR data, mobile LiDAR data requires a multi-step post-processing process to ensure data quality and perform multi-epoch change detection and deformation analysis.

Step 1: Although the SLAM-engine processes data in a real-time fashion while data is collected, most systems can or must use a secondary, offline SLAM-process to improve data quality and produce a point cloud file. Most of this process takes place without significant user input, but SLAM-parameters can be adjusted for specific use-cases, and collected data sets can be re-processed in the SLAM-engine to optimize results.

Step 2: After initial online and offline pre-processing, a point cloud file of the scanned environment can be exported for optional processing steps such as registration, cropping, sub-sampling, and filtering. While absolute registration positions the LiDAR data in a global reference frame, such as a Cartesian coordinate system of a survey map, relative registration is achieved by co-registering data of a scene to another data set of the same scene. Co-registration of a scan epoch to a previously recorded epoch is usually performed using the iterative closest point (ICP) algorithm (Besl and McKay, 1992).

When registering static and SLAM-based LiDAR data without global reference, particularly in confined underground excavations, drift error (i.e., incorrect translation and rotation) requires additional processing to remove to maintain data trueness and precision. The magnitude of drift increases with increasing scan trajectory length. As drift errors can lead to false-negative or positive change detection or deformation results, Jones et al. (2018) proposed the segmentation of MMS scans into sections that are then registered to a baseline scan. This process will improve precision and, in most cases, site-level trueness but can potentially obscure global changes. Some SLAM algorithms can register data sets without further segmentation by estimating the MMS's pose (i.e., position and orientation) in one scan epoch using data from another scan epoch of the same scene (Zhang and Singh, 2018). The quantification of SLAM-drift will help develop the appropriate collection, processing, and utilization workflows.

Step 3: Geotechnical monitoring results can be derived by change detection or deformation analysis. Change detection aims to provide a binary classification of points or objects within a scene into changed or unchanged (e.g., rockfall or shotcrete damage). In contrast, deformation analysis focuses on quantifying and potentially parameterizing changes – for example, for convergence monitoring applications. As described by Vosselman & Maas (2010), the complexity of monitoring methods increases with a decreasing signal-to-noise ratio in the data.

Table 1. Overview of LiDAR datasets that were utilized in this study.

Site / Instrument	Quality Level	Test	MMS Result Summary
Mine-A *Kaarta Stencil 2* *FARO Focus S70*	Target-Level	Visual detection	Similar detectability as static data
		Local trueness	1 cm range trueness bias
		Local precision	Within ±3 cm, less sharpness
		Coverage, density	Higher coverage, higher density
		Local averaging	M3C2 significantly increases precision
Edgar *Emesent Hovermap* *FARO x330*	Site-Level	Global Trueness	Within survey map trueness
		SLAM precision	0.02% variation of trajectory length

Step 1 SLAM-processing requires up to 250% of the time required for data collection. Processing time for Steps 2 and 3 primarily depends on the application and the required data quality. Changes can be detected a small area of interest within several minutes. Mine-scale monitoring benefits greatly from SLAM-based scan registration, which operates at a similar efficiency level as Step 1 processing. In ongoing work, we achieved same-day data collection and delivery of color-coded change maps for several kilometers of drift in an operating mine. The visual analysis of large, color-coded point clouds is currently still a time-consuming process.

2.5. Data Utilization

Lastly, change detection and monitoring process outputs need to be used in operational planning and decision making. For this, the availability, usability, and reliability of MMS data are vital considerations.

Understanding the data quality of MMS is essential during all stages of the workflow outlined above. Sofonia et al. (2019) suggested that mobile LiDAR data quality can be evaluated on a target and site level. Targets of a geotechnical monitoring campaign are any changes in the mine drift's surface that indicate geotechnically hazardous conditions such as rock block releases or a decrease in cross-sectional area. The target-level quality metrics that are considered most relevant for change detection and deformation analysis are high point cloud trueness, precision, coverage, and density. A "site" of a geotechnical monitoring campaign can be comprised of one or multiple underground entities such as drifts, stopes, ramps, or an entire mine. Important site-level LiDAR data quality metrics include global trueness, precision, and coverage.

3. METHODS

As shown in Table 1, this paper presents some of the data collected with two different MMSs (Kaarta Stencil 2, Emesent Hovermap) in two underground hard rock mines – one operational block caving mine (Mine-A) and the Colorado School of Mines Edgar Experimental Mine (Edgar). Data from Mine-A is used to evaluate the target-level quality, and data from Edgar is used to investigate site-level quality characteristics.

3.1. Instrumentation and Data Collection

Both systems used in this study represent the state-of-art in commercial mobile scanning and utilize a Velodyne Puck LiDAR sensor (Velodyne LiDAR, 2019) and IMU, as well as their respective proprietary SLAM algorithms. At Mine-A, a static FARO Focus S70 LiDAR operated by an experienced geotechnical engineer was utilized for ground truth measurements and to identify the differences between static and mobile point clouds.

Fig. 1. Mounting the Stencil 2 on a light mine utility vehicle.

We collected two data epochs at Mine-A with mobile Stencil 2 and the static FARO Focus S70 scanner to evaluate target-level data quality. To collect a pre-failure baseline epoch, we first deployed the Stencil 2 installed on an elevated position on the front roll bar tubing of a mine buggy (Figure 1). Then forwards and backward passes were performed at 8 km/h driving speed in a typical 70 m long section of the mine's extraction level. Additionally, a total of 4 static scan stations were chosen in the 70 m long test area. The scan duration (2 minutes/scan) and scan station position were chosen based on operator experience to replicate typical monitoring practices. After simulating the spalling of shotcrete on a mine pillar, the above process was repeated with both systems to collect a second "post-failure" epoch.

To evaluate site-level data quality, we deployed the Emesent Hovermap at the Colorado School of Mines Edgar Experimental Mine. A handheld scan epoch was collected by entering the "Miami portal" and traversing the "Miami drift" for a total length of 200 m.

3.2. Target- and Site-Level Evaluation

Both of our MMSs utilize a proprietary SLAM-engine and software package for real-time and initial post-processing steps. Most of this process takes place without significant user input, but SLAM-parameters can be adjusted for specific use-cases. We utilized CloudCompare (2021) and Maptek PointStudio (2021) for secondary processing steps.

We performed the target level data evaluation by registering the static and MMS pre-failure epochs to their equivalent post-failure epochs. We then identified changes by calculating absolute cloud-to-cloud closest point distances and colorization thresholding. Point cloud density was calculated and visualized by calculating the volumetric density within a radius of 0.02 m.

We evaluated the site-level trueness and precision by re-processing the exact same LiDAR data in two independent SLAM runs using the proprietary SLAM-engine's standard presets. This yielded two separate point cloud files of the same scene and epoch. We then registered both point clouds to each other and transformed them to fit a survey map. Lastly, we computed the distances between both clouds' points to evaluate the impact of SLAM-precision degradation over the length of the trajectory.

4. RESULTS

The following sections investigate some of the relevant target- and site-level quality metrics of MMS data in the context of geotechnical change detection and monitoring.

4.1. Target-Level Data Quality

Figure 2 gives an example of a target level assessment of two epochs of static (b) and mobile (c) LiDAR points classified into unchanged (white) and changed (red) after simulating spalling of shotcrete (a). The spalled slap of shotcrete is approximately 60 cm in diameter and 18 cm thick and can be easily identified in both static and MMS LiDAR after calculating absolute distances between points of the pre- and post-failure epochs. The spalled shotcrete rubble on the drift floor is also clearly visible, and rock fragments as small as 6 cm can be identified in both sets. The MMS point cloud in Figure 2 (c) appears to render the scene with lower sharpness compared to the static data in (b).

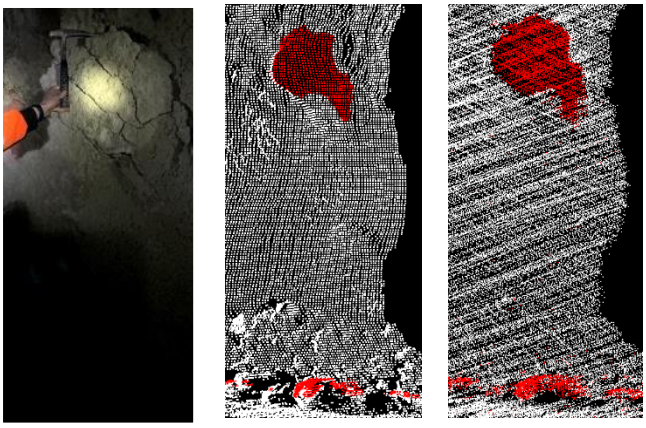

(a) (b) (c)

Fig. 2. Simulated spalling (a) and change detection on static (b) and MMS (c) LiDAR data.

Figure 3 illustrates a cross-section view of the same data set, focused on a flat target surface. Due to its range accuracy of ± 3 cm, the Velodyne Puck 16 LiDAR sensor generates point clouds with lower precision (i.e., higher deviation of points around the true object). 2D surfaces can therefore accumulate a 3D thickness and appear less sharp compared to static LiDAR data. Our tests also identified a systematic range trueness bias towards longer range measurements of the MMS. This can be observed in Figure 3, with the mean of the MMS points being shifted about 1 cm left to the actual surface.

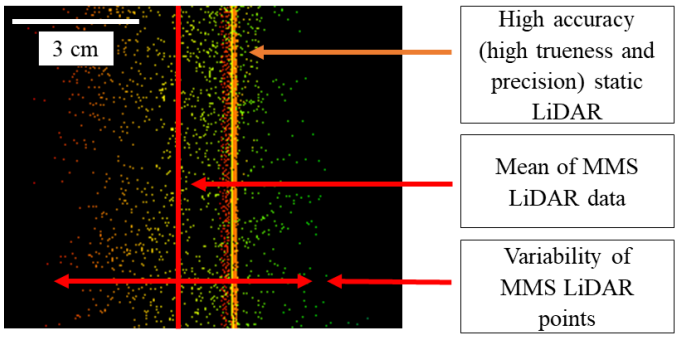

Fig. 3. Cross-section of a registered static and MMS point cloud representing a flat surface.

Although performing static LiDAR scanning based on best principles, a deterioration of coverage can be observed in Figures 4 (a) and (c). The closest scan station to the failure surface was located 5 m to the pillar's left, with the line-of-sight obscured by the pillar. With only one scan station covering the area of failure from 10 m away, the cloud's density is significantly lower on this side of the pillar. Although coverage is sufficient to delineate the failure, the static cloud density is highly variable even over this short interval. Figure 4 (c) shows a close-up view of the sparseness of the cloud. The MMS cloud in Figure 4 (b) provides good coverage of the mine pillar. Figure 4 (d) shows a significantly higher point density of MMS data than the static scanner.

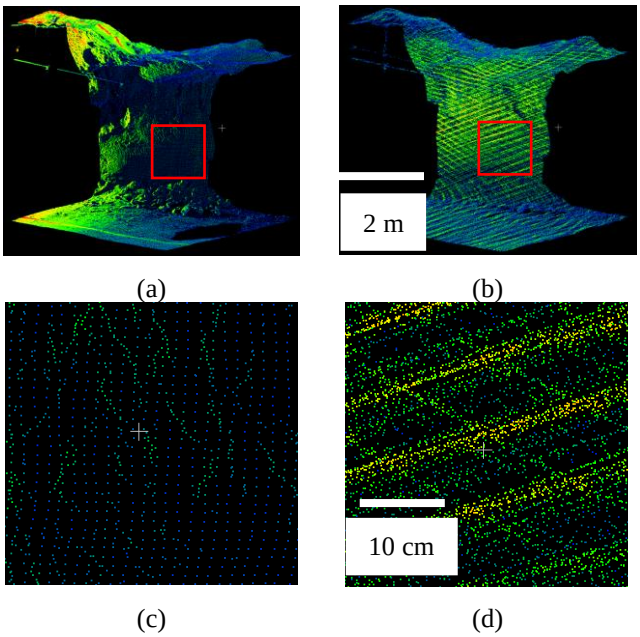

Fig. 4. Coverage and density difference between static (a, c) and MMS (b, d) point cloud data on a mine pillar.

The MMS point clouds' relatively uniform and dense nature can be exploited by averaging redundant data points to improve overall precision. Figure 5 illustrates an example of local averaging of noisy MMS LiDAR data by utilizing the Multiscale Model to Model Cloud Comparison (M3C2) described by Lague et al. (2013). The resulting point cloud resembles the high-precision static LiDAR point cloud, with improved sharpness and potentially better detectability of geotechnically relevant changes.

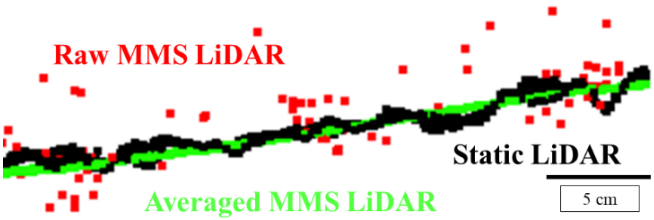

Fig. 5. Top view of a mine drift wall section. Low precision MMS LiDAR data can be effectively averaged with M3C2.

4.2. Site-Level Data Quality

The SLAM precision can be estimated by comparing the absolute distances between the two independent SLAM processing outputs of the same scan or of two independent scans. Performing the former, we investigate the variations in outputs caused by non-deterministic SLAM behavior. At the beginning of a given scan, SLAM precision is high, and only minimal differences exist between the two clouds. With increasing scan length, the SLAM algorithm generates a slightly different solution resulting in increasing differences between the two outputs. Based on the scan length of about 200 m and an average difference of 4 cm, the data shows variations of approximately 0.02 % of trajectory length. The point cloud's site-level trueness is within the survey base-map resolution of approximately 30 cm. (Figure 6)

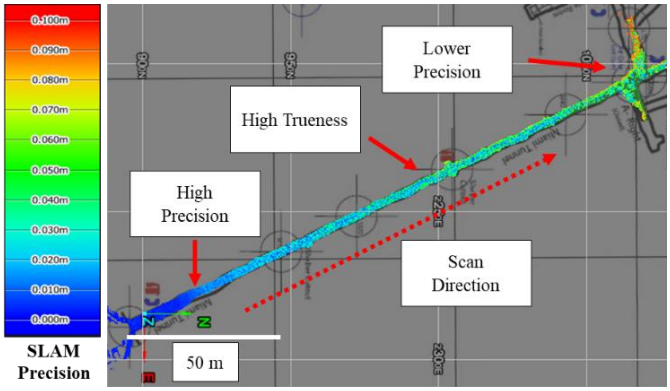

Fig. 6. Evaluation of SLAM precision and trueness over a 200 m long section of the Miami drift at the Edgar Mine.

In addition to the MMS LiDAR scans presented in this paper, we carried out static LiDAR scans. Due to the drift's small cross-section area (2 x 2 m), scan stations had to be spaced very closely (about every 10 m). The higher number of scan stations resulted in a much longer data collection time of approximately 1.5 h using a 3 min scan duration, compared to approximately 5 min for collection and 15 min for post-processing of the MMS data.

5. CONCLUSION

Workflows for collection and processing with current generation compact MMS are very similar to traditional static LiDAR but offer some key advantages – most notably speed and ease of data collection and processing. MMS data collection at Mine-A was conducted in real-time as part of a regular visual inspection of the whole extraction panel. Within 45 minutes, the team could scan and inspect 2.5 km of drift and deliver first point clouds within the same day. Data collection for the same area with a static LiDAR can take 2 – 3 full days (not including data processing to co-register individual scans). As we showed for smaller and more complex mine openings (Edgar), this time can increase significantly due to the closer spacing between scan stations. Therefore, MMSs enable data collection with no interruption of normal operations and minimal exposure of personnel to potentially hazardous conditions – a key hurdle for the use of static LiDAR for frequent, mine-wide monitoring.

The ability to utilize MMS LiDAR data for mine-wide geotechnical change detection depends highly on the target and site-level quality metrics trueness, precision, coverage, and point density. This study showed that despite the lower precision of current MMS raw data compared to static LiDAR data, very similar change detection results can be achieved when monitoring for discrete failure events such as roof fall, rib spalling, or skin failure.

Our tests also revealed a systematic range bias of the tested Stencil 2, most likely caused by the ranging-

accuracy limitation (lower trueness and precision than static LiDAR) of the Velodyne sensor. Although problematic when comparing LiDAR data from different mobile or static systems, the change detection quality is not affected by such systematic and, in our case, consistent biases.

In our tests, MMS data can provide better coverage, less occlusion, and a more uniform point density in confined mine drifts. This can increase the detectability of discrete failures by decreasing "blind spots" and hazardous false-negative change detection results.

We showed that local averaging techniques such as the popular but computationally expensive M3C2 algorithm could exploit the redundancy of MMS data and further improve its precision. Fundamentally, local averaging can aid in deformation monitoring of elastoplastic rock mass deformations (convergence), which typically requires lower signal-to-noise ratios than monitoring discrete failure targets.

The global data quality review showed the effect of SLAM processing drift on data quality. In practice, this will limit the maximum trajectory length before further post-processing workflows are required to maintain sufficient precision and trueness. Segmentation or SLAM-localization-based post-processing approaches can suppress drift. However, in doing so, they potentially obscure global deformation trends and introduce an additional computational cost. MSSs with higher SLAM precision enable longer data collection segments, reducing the processing effort and enabling a more reliable global deformation analysis.

6. RECOMMENDATIONS

SLAM-based mobile LiDAR scanning is currently in its infancy for mine-wide geotechnical monitoring applications. However, the various upsides and potential solutions for current limitations make this technology a promising alternative or supplement to traditional geotechnical monitoring and an exciting research area.

The following three areas will require further research to improve the proliferation of MSS into mining operations:

(i) A more detailed investigation of trueness and precision of SLAM-based LiDAR for low signal-to-noise ratio monitoring tasks

(ii) Investigation of local averaging techniques for geotechnical monitoring applications

(iii) Development of a purpose-built data utilization framework for frequent mine-wide MMS deployment and automation of monitoring

ACKNOWLEDGEMENTS

This work was funded by the National Institute of Occupational Safety and Health. (NIOSH) under Grant Number 200-2016-90154.

Fieldwork was made possible and supported by Mine-A and the Edgar Experimental Mine.

We would also like to acknowledge the support of the two MMS instrumentation partners Mine Vision Systems that provided a Kaarta Stencil 2 and Emesent that provided a Hovermap.

REFERENCES

1. Besl, P.J., McKay, N.D., 1992. A Method for Registration of 3-D Shapes. IEEE Trans. Pattern Anal. Mach. Intell. https://doi.org/10.1109/34.121791
2. CloudCompare, 2021. CloudCompare.
3. Emesent, 2021. Hovermap [WWW Document]. URL https://www.emesent.io/products/hovermap/
4. Fairhurst, C., 2017. Some Challenges of Deep Mining. Engineering 3, 527–537. https://doi.org/10.1016/J.ENG.2017.04.017
5. International Organization for Standardization, 2021. ISO 5725.
6. Jones, E., Ghabraie, B., Beck, D., 2018. A method for determining field accuracy of mobile scanning devices for geomechanics applications. ISRM Int. Symp. - 10th Asian Rock Mech. Symp. ARMS 2018 978–981.
7. Jones, E., Sofonia, J., Canales, C., Hrabar, S., Kendoul, F., 2020. Applications for the Hovermap autonomous drone system in underground mining operations. J. South. African Inst. Min. Metall. 120, 24–25. https://doi.org/10.17159/2411-9717/862/2020
8. Kaarta, 2021. Kaarta Products [WWW Document]. URL https://www.kaarta.com/products/stencil-2-for-rapid-long-range-mobile-mapping/
9. Kaiser, P.K., Cai, M., 2012. Design of rock support system under rockburst condition. J. Rock Mech. Geotech. Eng. https://doi.org/10.3724/sp.j.1235.2012.00215
10. Lague, D., Brodu, N., Leroux, J., 2013. Accurate 3D comparison of complex topography with terrestrial laser scanner: Application to the Rangitikei canyon (N-Z). ISPRS J. Photogramm. Remote Sens. https://doi.org/10.1016/j.isprsjprs.2013.04.009
11. Maptek, 2021. PointStudio.
12. Mark, C., Molinda, G.M., 2004. Preventing falls of ground in coal mines with exceptionally low-strength roof: two case studies, in: 23rd International Conference on Ground Control in Mining.
13. Nordlund, E., 2013. Deep hard rock mining and rock mechanics challenges, in: Ground Support 2013.
14. Palei, S.K., Das, S.K., 2008. Sensitivity analysis of

support safety factor for predicting the effects of contributing parameters on roof falls in underground coal mines. Int. J. Coal Geol. https://doi.org/10.1016/j.coal.2008.05.004

15. Sandbak, L.A., Rai, A.R., 2013. Ground support strategies at the turquoise ridge joint venture, Nevada, in: Rock Mechanics and Rock Engineering. https://doi.org/10.1007/s00603-012-0342-y

16. Sofonia, J.J., Phinn, S., Roelfsema, C., Kendoul, F., Rist, Y., 2019. Modelling the effects of fundamental UAV flight parameters on LiDAR point clouds to facilitate objectives-based planning. ISPRS J. Photogramm. Remote Sens. 149, 105–118. https://doi.org/10.1016/j.isprsjprs.2019.01.020

17. Velodyne LiDAR, 2019. Velodyne LiDAR "Puck" LITE Light Weight Real-Time 3D LiDAR Sensor: Product Specification [WWW Document]. URL https://velodynelidar.com/products/puck-lite/

18. Vosselman, G., Maas, H.-G., 2010. 7. Engineering Applications. Airborne Terr. Laser Scanning.

19. Zhang, J., Singh, S., 2018. Laser–visual–inertial odometry and mapping with high robustness and low drift. J. F. Robot. 35, 1242–1264. https://doi.org/10.1002/rob.21809

20. Zlot, R., Bosse, M., 2014. Efficient Large-Scale 3D Mobile Mapping and Surface Reconstruction of an Underground Mine, in: Yoshida, K., Tadokoro, S. (Eds.), Field and Service Robotics: Results of the 8th International Conference. Springer Berlin Heidelberg, Berlin, Heidelberg, pp. 479–493. https://doi.org/10.1007/978-3-642-40686-7_32